

R. Akkerman, H.W. Wiersma & L.J.B. Peeters
University of Twente, the Netherlands

ABSTRACT: Thermal and chemical shrinkage lead to distortions of continuous fibre reinforced thermoset laminates. Enclosed angles decrease after a hot cured composite component is released from the mould after cooling to ambient temperature. This is referred to as the spring-forward phenomenon. Usually, spring-forward is mainly caused by anisotropic thermal expansion, but this cannot explain totally the experimentally observed spring-forward. The effects of an inhomogeneous fibre/matrix distribution through the thickness, an inhomogeneous heat distribution during the cure-cycle and the difference in thermal expansion between the mould and the composite component are investigated.

1 INTRODUCTION

Continuous fibre reinforced thermoset laminates that are cured hot, exhibit deformations due to thermal and cure shrinkage. Residual stresses will develop in laminates due to the mismatch of thermal expansion along and across the fibres, cure shrinkage of the thermoset resin and the change from cure to room temperature. This leads to undesirable shape distortions when the cured components are released from the mould. The tool designer can accommodate for these distortions based on experience. This indicates that it is desirable to be able to predict these distortions, reducing trial and error time when producing a new component.

A particular shape distortion is the decrease of the enclosed angle in a corner of a composite component, what is usually referred to as the spring-forward phenomenon. Experiments, done by Hamamoto (1986), show that the spring-forward cannot be explained only by the mismatch in thermal expansion along and across the fibres. Nelson & Cairns (1989) have looked qualitatively at other possible causes of the spring-forward, like chemical shrinkage of the thermoset matrix and residual stresses at the full cure temperature.

In this paper a number of possible causes of the spring-forward in L-shaped parts are examined in detail. First, the main cause, mismatch in thermal expansion along and across the fibres, will be analysed together with the effect of an inhomogeneous fibre/matrix distribution through the thickness. Then, the model will be extended to

analyse the effects of the heat distribution, the chemical shrinkage and the thermal expansion of the mould during the cure cycle on the spring-forward.

2 THERMO-ELASTIC MODEL

2.1 Analysis

It is a common assumption that no stresses are built up in a laminate prior to completion of curing; which implies that stresses will only be generated during cool-down from cure to room temperature. Starting from the thermo-elastic approach of Kollar & Springer (1992) the thermally induced deformations in thick laminated corners were calculated (similar to Jain & Mai, 1997).

To this end, a thick-walled laminated composite cylinder segment (Fig. 1) was analysed (Wiersma et al, 1997). The three-dimensional orthotropic elasticity equations in cylindrical coordinates are

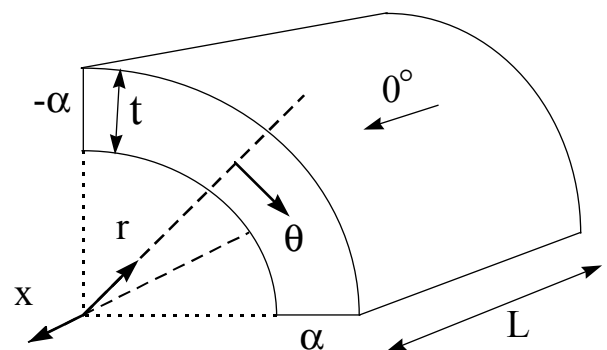


Figure 1. Cylindrical segment for distortion analysis

used to solve the displacement field, assuming the stresses and strains depend only on the radial coordinate. This leads to the following displacement field of one layer:

$$\begin{aligned}
 u_x &= c_1 x + c_2 \theta, \\
 u_\theta &= c_3 x r + c_4 \theta r, \\
 u_r &= A_1 \left| \frac{r}{R} \right|^{\delta_0} + A_2 \left(\frac{r}{R} \right)^{-\delta_0} \\
 &\quad - \delta_1 + \delta_2 R f_0(r) + \delta_3 R^2 f_1(r)
 \end{aligned} \quad (1)$$

With a suitable choice of boundary conditions for the laminate and continuity conditions between the individual layers this leads to a system of $2n+4$ equations for the same number of unknowns. The spring-forward is derived from the solution of this displacement field.

The model and its assumptions have been verified by a three-dimensional finite element calculation of the thermally induced deformation of a thick walled L-shaped laminate (Fig.2). The spring-forward calculated with the thermo-elastic model was within 2% of the result of the finite element simulation.

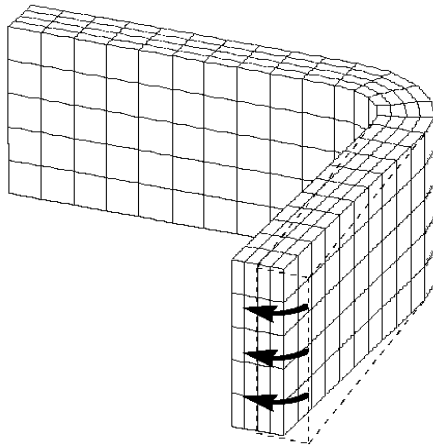


Figure 2. 3D Finite element verification of the thermo-elastic model using layered 8-node brick elements.

2.2 Results thermo-elastic model

A sensitivity analysis was performed to determine the parameters that have the largest influence on the spring-forward. The coefficient of thermal expansion (CTE) across the fibres and the stress-free temperature are the most important parameters. The ratio of radius versus thickness, R/t , determining whether a segment is thick-walled, is of little influence. Only with very low ratios, much lower than the condition for thin-walled corners, $R/t > 10$, there is an effect on the spring-forward. The stresses in the radial direction are small compared to the in-plane stresses with common thick-walled corners. The results of the thermo-elastic model for different L-shaped laminates are listed in Table 1. They are compared to the experimental results found by Fokker Aircraft B.V. (Voerman, 1992).

Table 1. Thermo-elastic model predictions versus experimental spring-forward results. Inner radius 5 mm, thickness 4 mm.

LAMINATE LAY-UP	SPRING-FORWARD		
	T-E model	male mould	female mould
$(90^\circ_{32})_T$	0.51°	0.83°	-
$(Y/0^\circ/X)_{\text{sym}}$	0.75°	1.29°	1.43°
$(X/Y/Z/X)_{\text{sym}}$	0.75°	1.22°	1.37°
$(Y/0^\circ/X/Y/Z/X)_{\text{sym}}$	0.75°	1.24°	1.35°

type X: $(+45^\circ/90^\circ/-45^\circ)$, Y: $(-45^\circ/90^\circ/+45^\circ)$, Z: $(0^\circ/0^\circ)$

The material used for the experiments is Ciba 6376C HTA Carbon/Epoxy Unidirectional tape with a curing temperature of 177°C . The stress-free temperature was measured to be 185°C , by heating up a cured unsymmetric laminate until it is complete flat again (Hahn & Hwang, 1983). A constant difference of 40% is observed between the calculated spring-forward and the measured spring-forward for specimens produced on a male mould. The spring-forward measured for specimens produced on a female mould is 45% larger than the calculated spring-forward. This implies that the spring-forward can not be predicted with the thermo-elastic model only. When reheating the specimens to the stress-free temperature, it was observed that there was not a total return of the spring-forward. Irreversible effects must therefore play a role.

2.3 Inhomogeneous fibre/matrix distribution

In the thermo-elastic model it was assumed that the different layers of the segment have equal thicknesses and a homogeneous fibre/matrix distribution. However, this is mostly not the case in corners of L-shaped parts. Specimens produced on a male mould usually have thinner corners, see Figure 3. On the other hand, specimens produced on a female mould usually have thicker corners, due to resin flow during the gelling period of the thermoset resin. This means that there will be a changing distribution of fibres and matrix through the corner. This will give different properties through the thickness of the corner, which will affect the spring-forward.

Cross-sections of corners were analysed by microscopy. An estimation of the fibre volume fraction through the thickness was made. Corners produced on a male mould showed a higher but

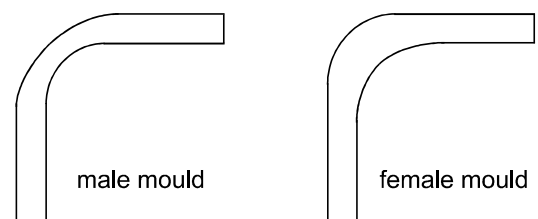


Figure 3. Change of laminate thickness in corners

homogeneous fibre volume fraction through the thickness. Corners produced on a female mould showed only a lower fibre volume fraction at the inside of the corner. By calculating the properties for every layer as a function of the fibre volume fraction the effect of a different distribution can be simulated. The thermo-elastic model was modified by changing the coefficients of thermal expansion due to the change in fibre volume fraction.

Simulations for corners produced on a female mould showed an increase of about 15% on the spring-forward of the homogeneous corner. It can however not explain the difference between the thermo-elastic model and the experiments. For corners made on male mould a decrease of 10% in spring-forward was calculated compared to the homogeneous corner. The calculated difference in spring-forward between specimens produced with a male and a female mould was confirmed by the experimental results from Fokker Aircraft B.V.

3 EXTENDED MODEL

With the thermo-elastic model only elastic (reversible) behaviour resulting in spring-forward has been considered. This could not explain the total spring-forward as found by the experiments. Therefore, irreversible effects that occur during the cure-cycle have been studied on the influence of spring-forward.

The polymerisation reaction of a thermoset resin is exothermic. The generated exothermic heat during the cure-cycle may cause substantial through thickness temperature gradients in the laminates. In turn, temperature gradients cause curing gradients which result in deformation gradients and in the development of additional residual stresses. Such residual stresses can contribute to the spring-forward of an L-shaped part. The cure-cycle has to be modelled to study the effect of an inhomogeneous heat distribution during the cure-cycle.

The thermosetting reaction further leads to chemical shrinkage. When the resin is in its liquid phase, this will not lead to stress build-up, but the contrary is true when the material is in a solid state. In between, stress relaxation will take place, to some extent. Chemical shrinkage will have an effect on the distortion of the component, increasing with the relaxation times of the curing resin.

The composite components considered here are cured in an autoclave on a male or a female mould. These moulds are usually made out of steel or aluminium. The moulds expand and contract due to the change in temperature during the cure-cycle. The composite components are thus subjected to deformations during the cure-cycle which can be irreversible and therefore can contribute to the spring-forward. By modelling the thermoset matrix

as a viscoelastic material the influence of both the chemical shrinkage and the expansion of the mould during the cure-cycle can be studied.

3.1 Thermal model

The thermosetting reaction leads to heat generation, which is included in the heat balance:

$$\dot{q} + \nabla \cdot (\mathbf{k} \cdot \nabla T) = \rho c_p \frac{\partial T}{\partial t} \quad (2)$$

The parameters \mathbf{k} , ρ and c_p are, respectively, the thermal conductivity tensor, density and specific heat of the composite. These thermal properties are assumed to be constant during the curing process in order to simplify the problem. The internal heat generation term, \dot{q} , accounts for the exothermic polymerisation reaction:

$$\dot{q} = \rho H_r \dot{\psi} \quad (3)$$

The heat of reaction, H_r , is the total heat released per unit mass for a completely cured laminate and $\dot{\psi}$ is the instantaneous rate of cure. The rate of cure can be modelled by using the following equation described by Bogetti & Gillespie (1992):

$$\dot{\psi} = A_c \exp\left|\frac{-\Delta E_c}{RT}\right| \psi^{m_c} (1-\psi)^{n_c} \quad (4)$$

where the parameter R denotes the universal gas constant and ΔE_c the activation energy. Further, m_c , n_c and A_c are dimensionless constants.

3.2 Mechanical model

We consider a composite consisting of a viscoelastic thermoset matrix and elastic continuous fibres. This composite is subjected to a cure-cycle. The thermoset matrix will exhibit a change in modulus and viscosity during this cycle, compared to which the changes in properties of the fibres are negligible. A homogeneous layer thickness and fibre/matrix distribution is assumed in the composite during the cure-cycle. Also, it is assumed that the matrix and fibres show only affine deformation: the fibre volume fraction remains constant during the cure-cycle.

The viscoelastic behaviour of the composite is described by characterising the fibre as an elastic spring and the matrix as a Maxwell element, consisting of an elastic spring and a viscous damper (only working on deviatoric deformations):

$$\begin{aligned} \boldsymbol{\varepsilon}_f &= \frac{1}{2G_f} \boldsymbol{\sigma}_f^d + \frac{1}{3K_f} \text{tr}(\boldsymbol{\sigma}_f) \mathbf{I} \\ &\equiv \underline{\underline{E}}_f^{-1} : \boldsymbol{\sigma}_f \\ \dot{\boldsymbol{\varepsilon}}_m &= \frac{1}{2G_m} \dot{\boldsymbol{\sigma}}_m^d + \frac{1}{3K_m} \text{tr}(\dot{\boldsymbol{\sigma}}_m) \mathbf{I} + \frac{1}{2\eta} \boldsymbol{\sigma}_m^d \\ &\equiv \underline{\underline{E}}_m^{-1} : \dot{\boldsymbol{\sigma}}_m + \underline{\underline{C}} : \boldsymbol{\sigma}_m \end{aligned} \quad (5^{a,b})$$

where $\boldsymbol{\varepsilon}$ and $\boldsymbol{\sigma}$ are the linear strain and stress tensor respectively, superscript d denotes the deviatoric part, \mathbf{I} is the unit tensor, G and K are, respectively, the shear and bulk modulus, η is the viscosity, $\underline{\underline{E}}$ and $\underline{\underline{C}}$ are, respectively, the fourth order elasticity and creep tensor. The connection between both components is made by simple Rules of Mixtures (to start with the simplest approximation): equal strains in the fibre direction, equal stresses in the transverse directions, resulting in e.g.

$$\begin{aligned}\sigma_1 &= V_f \sigma_{f,1} + (1 - V_f) \sigma_{m,1} \\ \dot{\varepsilon}_2 &= V_f \dot{\varepsilon}_{f,2} + (1 - V_f) \dot{\varepsilon}_{m,2}\end{aligned}\quad (6^{a,b})$$

A unidirectional layer is thus modelled by a combination of an elastic spring and a Maxwell element. Figure 4 shows a simplified representation (neglecting Poisson's ratio effects) of the combination of the elements for the longitudinal and the transverse direction of the unidirectional layer.

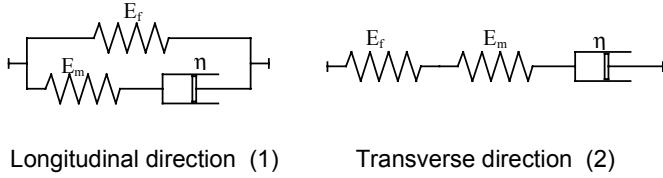


Figure 4. Composite model with fibre and matrix elements

Formally, the equations can be elaborated to a relation between stress and strain tensors. Here, we use a matrix-vector formulation to find a first order system of o.d.e.'s for the stress vector (denoted by brackets),

$$\{\dot{\boldsymbol{\sigma}}\} = -[\mathbf{E}] \cdot [\mathbf{C}] \cdot \{\boldsymbol{\sigma}\} + [\mathbf{E}] \cdot \{\dot{\boldsymbol{\varepsilon}}\} - [\mathbf{E}] \cdot [\mathbf{R}] \cdot \{\boldsymbol{\varepsilon}\} \quad (7)$$

where $[\mathbf{E}]$ is the usual stiffness matrix for orthotropic materials, $[\mathbf{C}]$ is a non-symmetric creep matrix and $[\mathbf{R}]$ is a retardation matrix, related to the creep matrix:

$$[\mathbf{C}] = \begin{bmatrix} c_{11} & c_{12} & c_{12} & 0 & 0 & 0 \\ c_{21} & c_{22} & c_{23} & 0 & 0 & 0 \\ c_{21} & c_{23} & c_{22} & 0 & 0 & 0 \\ 0 & 0 & 0 & c_{44} & 0 & 0 \\ 0 & 0 & 0 & 0 & c_{44} & 0 \\ 0 & 0 & 0 & 0 & 0 & c_{44} \end{bmatrix}, \quad (8)$$

$$[\mathbf{R}] = -V_f E_f \begin{bmatrix} c_{11} & 0 & 0 & 0 & 0 & 0 \\ c_{21} & 0 & 0 & 0 & 0 & 0 \\ c_{21} & 0 & 0 & 0 & 0 & 0 \\ 0 & 0 & 0 & 0 & 0 & 0 \\ 0 & 0 & 0 & 0 & 0 & 0 \\ 0 & 0 & 0 & 0 & 0 & 0 \end{bmatrix},$$

which contain the following terms:

$$\begin{aligned}c_{11} &= \frac{E_m^*}{3\eta}, \\ c_{12} &= -\frac{E_m^*}{6\eta} \left(1 - (1 - 2\nu_f) V_f \right), \\ c_{21} &= -\frac{1}{6\eta} \left(1 - 2V_f \left(\nu_f E_m^* - \nu_m E_f^* \right) \right), \\ c_{22} &= \frac{1}{6\eta} \left[\begin{array}{l} (1 - 2\nu_m) V_f \nu_f \\ + (2 - \nu_m) V_m \end{array} \right] V_f E_f^* + \left[\begin{array}{l} 2V_f^2 \nu_f^2 \\ + 2V_f V_m \nu_f + 2V_m^2 \end{array} \right] E_m^*, \\ c_{23} &= \frac{1}{6\eta} \left[\begin{array}{l} \left((1 - 2\nu_m) V_f \nu_f \right) \\ - (1 + \nu_m) V_m \end{array} \right] V_f E_f^* + \left[\begin{array}{l} 2V_f^2 \nu_f^2 \\ + 2V_f V_m \nu_f - V_m^2 \end{array} \right] E_m^*, \\ c_{44} &= \frac{V_m}{\eta}, \\ E_f^* &= \frac{E_f}{V_f E_f + V_m E_m}, \\ E_m^* &= \frac{E_m}{V_f E_f + V_m E_m}.\end{aligned}\quad (9)$$

With this constitutive relationship the behaviour of a unidirectional layer during the cure-cycle is described.

The moduli are assumed to be constant during the cure-cycle, only the relaxation times change due to curing and temperature changes (thermo-rheologically simple behaviour). The stress-strain relations can easily be put into a discrete form using a forward Euler scheme, to be used in subsequent finite element calculations. However, the stability of explicit schemes is limited by the relaxation times, resulting in a huge number of time steps required to obtain a convergent solution for a complete cure cycle. A solution to this problem is to solve the stress-strain relations analytically for a constant strain rate, as in Akkerman (1993), using standard theory of ordinary differential equations. First the homogeneous system for the stress rate is solved using the initial stress state, then the particular solution is obtained using the state of strain changing linearly with time. Addition of both terms leads to the analytical solution, which is a linear relation between stress increment, initial stress and strain and the strain increment,

$$\begin{aligned}\{\Delta \boldsymbol{\sigma}\} &= -[\mathbf{E}] \cdot [\mathbf{C}^*] \cdot \{\boldsymbol{\sigma}_0\} + [\mathbf{E}] \cdot \{\Delta \boldsymbol{\varepsilon}\} \\ &\quad - [\mathbf{E}] \cdot [\mathbf{R}^*] \cdot \{\boldsymbol{\varepsilon}_0\}\end{aligned}\quad (10)$$

Here, the incremental strain vector consists of three terms: thermal strain, curing strain and mechanical strain. When the system is behaving completely elastic (infinite viscosity) then the creep and

recovery matrices are zero. Only the coefficients in the “time-integrated creep and recovery matrices” depend on the current temperature and degree of cure. This discretisation has good stability properties for all timesteps. It is suitable for implementation within a finite element program, together with the viscosity relation, degree of cure relation and heat conduction equation.

The most important changing parameter is now the viscosity (proportional to the relaxation time) of the thermoset matrix, because the elastic properties are kept constant during the cure-cycle. A simple viscosity relation depending on temperature and degree of cure is used (Bruschke & Advani, 1994):

$$\eta(T, \psi) = \eta_0 \exp \left| \frac{U_{act}}{RT} + k_v \psi^{m_v} \right| \quad (11)$$

where η_0 is a reference viscosity, U_{act} the activation energy, R the universal gas constant, T the temperature, ψ the degree of cure and k_v and m_v are curing constants. The viscosity can be measured until the gel-point is reached, after this the cross-link reaction has reached too far to define a viscosity. The interesting area of viscosity, with respect to stress development, is however before the gel-point.

3.3 Finite element analysis

The models have been implemented in the thermo-mechanically coupled finite element package DIEKA, developed at the Department of Mechanical Engineering of the University of Twente. The heat conduction in the composite is assumed to be isotropic for simplicity, although conduction along the fibres is in reality higher than the conduction across the fibres. The heat conduction coefficient in the direction across the fibres is taken as the isotropic conduction coefficient. The heat transfer between the laminate and the mould is assumed to be perfect. The material property data used for the simulations are listed in Table 2.

A cross-section of a unidirectional L-shaped laminate on a steel male mould was modelled, see Figure 5. Linear quadrilateral elements (generalised plane strain) were used for the simulation. The laminate thickness is 4 mm and the inner radius is 5 mm. Only a half of the corner was modelled because of symmetry conditions. Mesh refinement showed no significant change in results.

Simulations were performed using the standard cure-cycle of Fokker Aircraft B.V. The temperature was prescribed at the boundary surfaces of the steel mould and the composite laminate corresponding to the cure-cycle. The laminate is assumed to be connected to the mould during the cure-cycle, no slip is allowed. After the cure-cycle simulation the laminate is still connected to the mould, resulting in internal stresses. The spring-forward is determined by disconnecting the laminate from the mould.

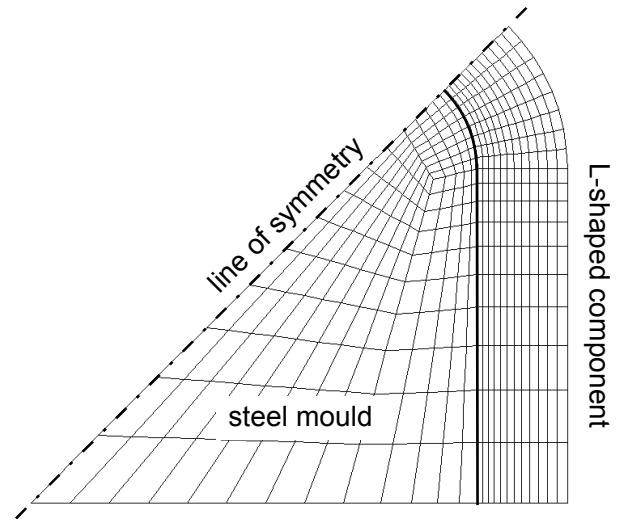


Figure 5. Finite Element representation of the moulding process.

Table 2. Material property data

Ciba 6367C resin			ud carbon-epoxy		
E	4.3	GPa	E_1	135	GPa
ν	.37		E_2	9.5	GPa
α	$76 \cdot 10^{-6}$	1°C	G_{12}	5.1	GPa
ρ	1507	kg/m^3	ν_{12}	0.3	
H_r	198	kJ/kg	ν_{23}	0.6	
A_c	3266		α_1	$0.3 \cdot 10^{-6}$	1°C
ΔE_c	56.6	kJ/mol	α_2	$35 \cdot 10^{-6}$	1°C
m_c	0.3		k_2	0.45	W/mK
n_c	1.0		ρ	1500	kg/m^3
ϵ_{cure}	-0.02	m^3/m^3	c_p	942	J/kgK
η_0	0.254	$\text{Pa}\cdot\text{s}$	V_f	0.66	
U_{act}	4690.59	J/mol	mould steel		
k_v	75.		E	210	GPa
m_v	2.5		ν	0.3	
HTA carbon fibre			α	$12 \cdot 10^{-6}$	1°C
E_1	230	GPa	k	60.5	$\text{W/m}^2\text{K}$
ν_{12}	.2		ρ	7833	kg/m^3
α_1	$-0.4 \cdot 10^{-6}$	1°C	c_p	434	J/kg K

4 RESULTS EXTENDED MODEL

The temperature gradients found, during the curing process, are so small that these will not affect the spring-forward. The maximum differences are about 0.3°C . Significant temperature gradients appear only with higher heating rates, e.g. $10^\circ\text{C}/\text{min}$, and very thick laminates, e.g. 25 mm thick. It can be concluded that temperature gradients, in the laminated products considered here, are too small to have a significant contribution to the spring-forward.

The relative spring-forward found, at the end of the simulation with the unidirectional laminate, is 0.68° . This is 33% larger than the spring-forward found with the elastic model, which is 0.51° . However, the spring-forward calculated is still

smaller than the spring-forward found experimentally by Voerman (1992), which was 0.83° , a difference of 22%. Care must be taken with interpretation of the simulation results because a simplified model is used with some data obtained from similar materials.

Table 3. Spring forward results from the extended model for the UD laminate, inner radius 5 mm, thickness 4 mm.

$\alpha_{\text{mould}} (1/^\circ\text{C})$	ϵ_{cure}	spring forward
$12 \cdot 10^{-6}$	2%	0.68°
$25 \cdot 10^{-6}$	2%	0.77°
0	2%	0.59°
$12 \cdot 10^{-6}$	1%	0.64°
$12 \cdot 10^{-6}$	0%	0.59°
0	0%	0.49°

The effects of thermal expansion of the mould and cure shrinkage were also studied (table 3). Simulations were performed with a zero CTE of the mould and a high CTE ($25 \cdot 10^{-6} / ^\circ\text{C}$), and with cure shrinkages of 2, 1 and 0%. Decreasing the CTE leads to a smaller spring-forward (0.59°), the high CTE results in a higher spring-forward (0.77°). The same amount of change in spring forward can be accomplished by changing the cure shrinkage from 2% to 0%. This indicates that both the thermal expansion of the mould and the cure shrinkage have a significant influence on the spring-forward, which agrees with the expectations of Nelson & Cairns (1989). When both the thermal expansion of the mould and the cure shrinkage are set to zero, the extended model gives approximately the value obtained from the thermo-elastic model. Both effects appear to be separable, as the spring-forward varies almost linearly with these parameters.

Apart from this, the predicted spring-forward is sensitive to the viscosity profile. The viscosity profile in the viscoelastic area around the gel-point has a large influence on the spring-forward, as this determines the point where the cure shrinkage becomes "effective". This indicates that viscoelastic behaviour of the composite during the cure-cycle is an important factor in the spring-forward.

5 CONCLUSION

Several influences on the spring-forward in continuous fibre-polymer L-shaped parts have been studied. For the material studied here, 60% of the spring-forward is caused by the mismatch in thermal shrinkage due to cooldown from the stress-free temperature to the ambient temperature. The remainder is caused by a combination of different effects. In this, chemical shrinkage, thermal expansion of the mould and the stiffness increase of the resin during cure play an important role.

With a fairly crude model for a curing resin, combined to composite properties by very simple rules of mixture, the approximation of the measured spring-forward is improved significantly. Further improvement can be expected by applying a more sophisticated description of the curing resin and the composite properties.

ACKNOWLEDGEMENTS

The authors would like to acknowledge the support of Fokker Aircraft B.V. for the contribution to the experimental work.

REFERENCES

- Akkerman, R. 1993. *Euler-Lagrange Simulations of Nonisothermal Viscoelastic Flows*. Ph.D. thesis University of Twente.
- Bogetti, T.A. & J.W. Gillespie 1992. Process-induced stress and deformation in thick-section thermoset composite laminates. *J. of Composite Materials*, 26:626-660.
- Bruschke, M.V. & S.G. Advani 1994. A numerical approach to model non-isothermal viscous flow through fibrous media with free surfaces. *Int. J. of Solids and Structures*, 19:575-603.
- Hahn, H.T. & D.G. Hwang 1983. Residual stresses and their effects in composite laminates, *Proc. of NCKU/AAS Int. Symposium on Engineering Sciences and Mechanics*, 1199-1214.
- Hamamoto, A. 1986. Curing deformation of L-shaped composite parts. *Proc. of the Int. Symposium on Composite Materials and Structures*, 1092-1097.
- Jain, L.K. & Y.-W. Mai 1997. Stresses and deformations induced during manufacturing; Part I: Theoretical analysis of composite cylinders and shells, *J. of Composite Materials*, 31:673-695.
- Kollar, L.P. and G.S. Springer 1992. Stress analysis of anisotropic laminated cylinders and cylindrical segments, *Int. J. of Solids and Structures*, 29:1499-1517.
- Nelson, R.H. & D.S. Cairns 1989. Prediction of dimensional changes in composite laminates during cure. *Int. SAMPE Symposium and Exhibition Book 2*, 2397-2410.
- Voerman, G.W. 1992. *Research on shape and dimensional stability of ribs and beams produced of thermoset composite material*. Internal publication Fokker Aircraft B.V.
- Wiersma, H.W., L.J.B. Peeters & R. Akkerman 1997. Prediction of spring-forward in continuous fibre-polymer L-shaped parts, *Composites A*, accepted.